

Double waveguide couplers produced by simultaneous femtosecond writing

Matthias Pospiech^{1*}, Moritz Emons¹, Andy Steinmann¹, Guido Palmer¹, Roberto Osellame³, Nicola Bellini³, Giulio Cerullo³ and Uwe Morgner^{1,2}

¹*Institute of Quantum Optics, Leibniz Universität Hannover, Welfengarten 1, D-30167 Hannover, Germany*

²*Laser Zentrum Hannover e.V., Hollerithallee 8, D-30419 Hannover, Germany*

³*Istituto di Fotonica e Nanotecnologie - CNR, Dipartimento di Fisica - Politecnico di Milano, P.zza Leonardo da Vinci 32, 20133 Milano, Italia*

*Corresponding author: pospiech@iqo.uni-hannover.de

Abstract: We report on a novel method to create waveguide coupler devices in fused silica by combining the technique of beam shaping with femtosecond laser writing. The method is based on a programmable phase modulator and a dynamic variation of the phase-pattern during the writing process. The major advantage is the possibility to create complex devices in a single sweep by simultaneously writing two or more waveguides with changing separation. The guiding properties and the coupling behavior between the waveguides are investigated.

© 2009 Optical Society of America

OCIS codes: (050.1950) Diffraction gratings; (070.6120) Spatial light modulators; (140.3300) Laser beam shaping; (230.7370) Waveguides; (250.5300) Photonic integrated circuits; (350.3390) Laser materials processing

References and links

1. K. Minoshima, A. M. Kowalevicz, E. P. Ippen, and J. G. Fujimoto, "Fabrication of coupled mode photonic devices in glass by nonlinear femtosecond laser materials processing," *Opt. Express* **10**, 645–652 (2002). <http://www.opticsexpress.org/abstract.cfm?URI=oe-10-15-645>.
2. A. M. Streltsov and N. F. Borrelli, "Fabrication and analysis of a directional coupler written in glass by nanojoule femtosecond laser pulses," *Opt. Lett.* **26**, 42–43 (2001). <http://ol.osa.org/abstract.cfm?URI=ol-26-1-42>.
3. R. Osellame, V. Maselli, N. Chiodo, D. Polli, R. M. Vazquez, R. Ramponi, and G. Cerullo, "Fabrication of 3D photonic devices at 1.55 μm wavelength by femtosecond Ti:Sapphire oscillator," *Electron. Lett.* **41**, 315–317 (2005).
4. D. Homoelle, S. Wielandy, A. L. Gaeta, N. F. Borrelli, and C. Smith, "Infrared photosensitivity in silica glasses exposed to femtosecond laser pulses," *Opt. Lett.* **24**, 1311–1313 (1999). <http://ol.osa.org/abstract.cfm?URI=ol-24-18-1311>.
5. S. Nolte, M. Will, J. Burghoff, and A. Tünnermann, "Femtosecond waveguide writing: a new avenue to three-dimensional integrated optics," *Appl. Phys. A* **77**, 109–111 (2003).
6. J. Liu, Z. Zhang, S. Chang, C. Flueraru, and C. P. Grover, "Directly writing of 1-to-N optical waveguide power splitters in fused silica glass using a femtosecond laser," *Opt. Commun.* **253**, 315–319 (2005). <http://www.sciencedirect.com/science/article/B6TVF-4G6J7BK-4/2/ede39cc51bbd43d00faaaa0733ae52c>.
7. C. Florea and K. A. Winick, "Fabrication and Characterization of Photonic Devices Directly Written in Glass Using Femtosecond Laser Pulses," *J. Lightwave Technol.* **21**, 246–253 (2003). <http://jlt.osa.org/abstract.cfm?URI=JLT-21-1-246>.
8. Y. Gu, J.-H. Chung, and J. G. Fujimoto, "Femtosecond Laser Fabrication of Directional Couplers and Mach-Zehnder Interferometers," in *Conference on Lasers and Electro-Optics/Quantum Electronics and Laser Science*

- Conference and Photonic Applications Systems Technologies*, p. CThS3 (Optical Society of America, 2007).
<http://www.opticsinfobase.org/abstract.cfm?URI=CLEO-2007-CThS3>.
9. R. R. Thomson, A. S. Bockelt, E. Ramsay, S. Beecher, A. H. Greenaway, A. K. Kar, and D. T. Reid, "Shaping ultrafast laser inscribed optical waveguides using a deformable mirror," *Opt. Express* **16**, 12,786–12,793 (2008).
<http://www.opticsexpress.org/abstract.cfm?URI=oe-16-17-12786>.
 10. C. Mauchair, A. Mermillod-Blondin, N. Huot, E. Audouard, and R. Stoian, "Ultrafast laser writing of homogeneous longitudinal waveguides in glasses using dynamic wavefront correction," *Opt. Express* **16**, 5481–5492 (2008).
<http://www.opticsexpress.org/abstract.cfm?URI=oe-16-8-5481>.
 11. A. Steinmann, G. Palmer, M. Emons, M. Siegel, and U. Morgner, "Generation of 9- μ J 420-fs Pulses by Fiber-Based Amplification of a Cavity-Dumped Yb:KYW Laser Oscillator," *Laser Phys.* **18**, 527–529 (2008).
 12. G. Palmer, M. Emons, M. Siegel, A. Steinmann, M. Schultze, M. Lederer, and U. Morgner, "Passively mode-locked and cavity-dumped Yb:KY(WO₄)₂ oscillator with positive dispersion," *Opt. Express* **15**, 16017–16021 (2007).
<http://www.opticsexpress.org/abstract.cfm?URI=oe-15-24-16017>.
 13. W. J. Reichman, D. M. Krol, L. Shah, F. Yoshino, A. Arai, S. M. Eaton, and P. R. Herman, "A spectroscopic comparison of femtosecond-laser-modified fused silica using kilohertz and megahertz laser systems," *Journal of Applied Physics* **99**, 123112 (pages 5) (2006).
 14. S. Eaton, H. Zhang, P. Herman, F. Yoshino, L. Shah, J. Bovatsek, and A. Arai, "Heat accumulation effects in femtosecond laser-written waveguides with variable repetition rate," *Opt. Express* **13**, 4708–4716 (2005).
<http://www.opticsexpress.org/abstract.cfm?URI=oe-13-12-4708>.
 15. C. Schaffer, J. Garcia, and E. Mazur, "Bulk heating of transparent materials using a high-repetition-rate femtosecond laser," *Appl. Phys. A* **76**, 351–354 (2003).
 16. L. Shah, A. Arai, S. Eaton, and P. Herman, "Waveguide writing in fused silica with a femtosecond fiber laser at 522 nm and 1 MHz repetition rate," *Opt. Express* **13**, 1999–2006 (2005).
<http://www.opticsexpress.org/abstract.cfm?URI=oe-13-6-1999>.
 17. L. P. Boivin, "Multiple Imaging Using Various Types of Simple Phase Gratings," *Appl. Opt.* **11**, 1782–1792 (1972).
 18. B. Apter, U. Efron, and E. Bahat-Treidel, "On the fringing-field effect in liquid-crystal beam-steering devices," *Appl. Opt.* **43**, 11–19 (2004).
 19. B. E. A. Saleh and M. C. Teich, *Fundamentals of Photonics* (John Wiley & Sons, 1991).
-

1. Introduction

Femtosecond laser irradiation in transparent materials is a powerful and straightforward method for the fabrication of optical waveguides. When a femtosecond laser pulse is tightly focused inside the bulk, the intensity in the focal volume becomes high enough to cause absorption through nonlinear processes, leading to a permanent refractive index modification after relaxation of the plasma. Under suitable irradiation conditions the refractive index change is positive, allowing direct fabrication of guiding structures. Using this technique, several integrated optical devices have been demonstrated, such as couplers [1, 2, 3], splitters [4, 5, 6], and interferometers [7, 8]. At present, such devices are fabricated in a serial way, which means that each waveguide is written after the other. However, photonic devices such as couplers or interferometers require a precise control over the relative positions of the parallel or overlapping structures.

Recently, the use of a Spatial Light Modulator (SLM) has been adopted in single waveguide writing to control the shape of the waveguide cross-section [9] or to compensate for spherical aberrations in longitudinal writing [10]. In this paper we introduce a novel technique, based on adaptive beam shaping of the femtosecond laser with a SLM, that allows the implementation of multiple foci with controlled power distribution and dynamically variable distance. We use this technique for the fabrication of complex integrated optical devices in a single sweep. In particular, we demonstrate multiple parallel waveguides and directional couplers.

2. Experimental setup

The experimental setup is shown in Fig. 1. A novel femtosecond Yb-fiber based amplifier [11] seeded with a cavity-dumped Yb:KYW laser oscillator [12] is employed. This system provides up to 9 μ J at 420 fs at a repetition rate of 1 MHz, which is more than enough to reach the

waveguide writing threshold in many foci simultaneously. With respect to lower repetition rate systems, femtosecond laser writing on several glasses with this high repetition rate in general gives rise to thermal diffusion and heat accumulation effects which lead to an increase in the waveguide diameter and an increase in the refractive index contrast, while reducing the waveguide losses [13, 14, 15]. In the present work a fused silica sample is employed; in this material heat accumulation has not been observed [14], but nevertheless a significant index change increase has been achieved [16].

The SLM is a liquid-crystal phase modulator (Hamamatsu PPM, model X8267-15) consisting of an array of 768×768 pixels with a pixel size of $\approx 26 \mu\text{m}$ and is addressed via computer control. The incident power can be varied by a $\lambda/2$ -plate and a polarizing beam splitter; the beam is expanded to a Gaussian radius of 8 mm so that the $20 \text{ mm} \times 20 \text{ mm}$ aperture of the SLM is almost filled. The SLM is inserted under a small angle, and the shaped laser beam is demagnified by a telescope in order to match the aperture of the final microscope objective.

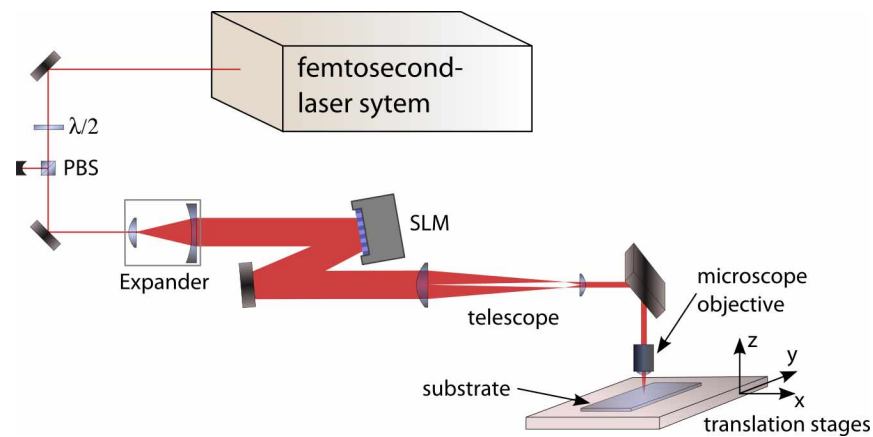


Fig. 1. Waveguide writing setup.

The fused silica sample is fixed to a computer-controlled 3D translation stage (Physik Instrumente M-511.DD in x -direction and M-505.2DG in y - and z -directions). Waveguide writing is performed along the x -direction with a speed ranging from 0.1 to 1 mm/s. The translation stages are mounted on a massive and rigid granite block to reduce vibrations from the environment.

The femtosecond laser pulses are tightly focused into the bulk of the sample using a $20\times$ microscope objective with a numerical aperture of $NA = 0.35$. The waveguides are written by moving the fused silica sample perpendicularly with respect to the laser beam axis. All structures are written inside the sample at a depth of approximately $150 \mu\text{m}$. The polarization is linear and parallel to the writing direction.

Multiple foci are created by applying to the SLM a periodic rectangular phase grating, which has the property to distribute the incident radiation in distinct diffraction orders. The separation (diffraction angle) of the diffracted orders is determined by the period of the phase grating. After a focusing lens the diffracted beams are translated into multiple foci in the focal plane, according to the 2D Fourier transform of the phase shaped laser beam. In our experiments, the grating period has a 50% duty cycle with an equal number of upper and lower phase pixels.

Diffraction of light into the distinct orders as a function of the phase contrast is pictured in Fig. 2. For a grating phase contrast of π , 80% is diffracted into the ± 1 orders [17], as also shown in Fig. 2. Alternatively, a three foci situation including the zero order can be accomplished with a grating contrast of 0.65π . The separation of the diffraction orders is determined by the grating

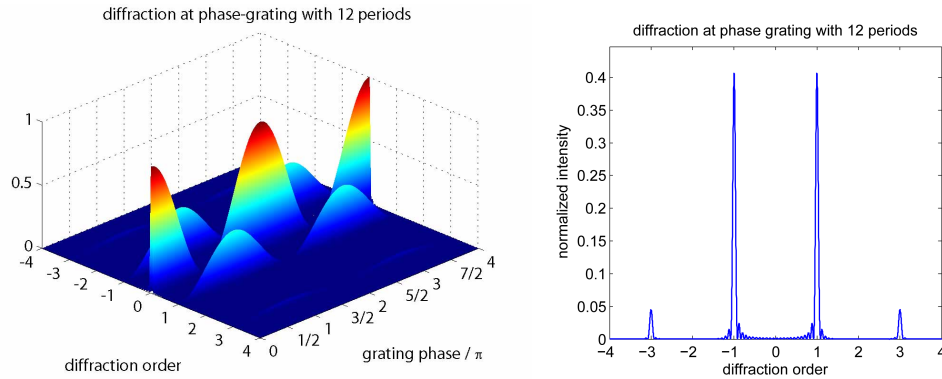


Fig. 2. Diffraction at rectangular phase grating for multiple periods. The left image shows the evolution of intensity in diffraction orders and the right one the separation into two foci at π -phase.

period.

Phase shapes with an imperfect phase progression may cause an incomplete removal of the zero order in the experiment. Nevertheless a careful calibration of the SLM can keep the amount of light in the zero order well below the material modification threshold, so that no additional blocking of the zero order at the intermediate focus is necessary.

3. Experimental results

3.1. Simultaneously written straight waveguide pairs

We first created simultaneously written waveguide pairs in fused silica by applying to the SLM a phase grating with a rectangular shape and a π -phase contrast. The translation speeds for waveguide writing ranged from 100 to 1000 $\mu\text{m/s}$. All presented results have been achieved with a pulse energy of 1.6 μJ . Taking the losses of the microscope objective ($\approx 25\%$) and the losses due to higher diffraction orders ($\approx 20\%$) into account this corresponds to 500 nJ per focus for a double structure. In Fig. 3 microscope images of these waveguide pairs are displayed.

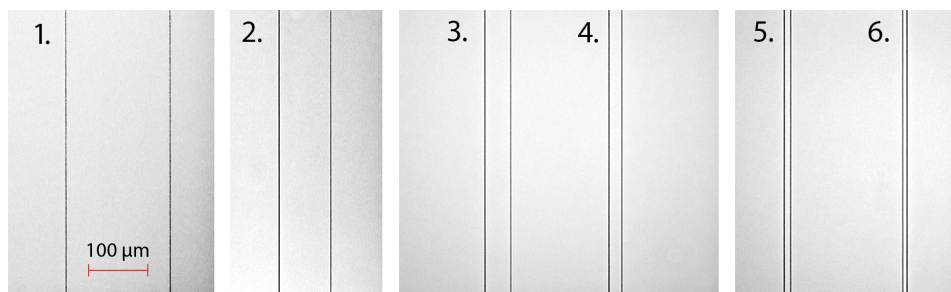


Fig. 3. 1) 175.3 μm (10 px), 2) 87.7 μm (20 px), 3) 43.8 μm (40 px), 4) 21.9 μm (80 px), 5) 11.0 μm (160 px), 6) 7.2 μm (240 px). The numbers in brackets indicate the phase grating period in pixels. The scaling is equal in all images.

Figure 4 illustrates the experimental distances between the two foci as a function of the grating period (full circles), as measured from the images reported in Fig. 3. The distance

between the waveguides varies from 175 μm to 7 μm for grating periods of 10 to 240 pixels. The data points almost perfectly match the theoretically calculated hyperbola.

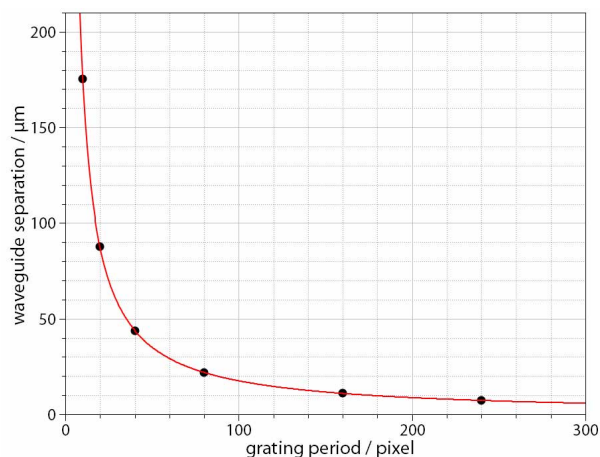


Fig. 4. Separation between double waveguides depending on the applied phase grating period. The separation was measured using the calibrated microscope images, see figure 3.

The maximum separation is limited by the smallest possible grating period – in our case 10 pixels (175 μm separation). Smaller periods lead to an increasing deviation between applied phase and the actual resulting phase mask, which significantly reduces the diffraction efficiency [18]. On the other side, the smallest possible separation is limited by the largest diffraction period available, which is the full aperture, meaning 768 pixels or 20 mm, which corresponds to a separation of 3.4 μm . The hyperbolic curve progression shows that for large grating periods the slope of the calibration curve is very small and thus a high accuracy in waveguide separation is achievable. The guiding properties of these waveguides were investigated by butt-coupling the light from an infrared fiber laser at 1550 nm (Santec, ECL-200) into one of the multiple waveguides and observing the guided modes with a Vidicon camera (Hamamatsu, C2400) at the output.

All waveguides are single-mode at 1550 nm. Figure 5 shows the near field of the guided mode of one of the two waveguides separated by 175 μm . We chose the maximum separation in order to characterize one waveguide independently from the other. The mode field diameter (full width at $1/e^2$) is around 15 μm in x - and 14 μm in z -direction. In the two right panels of Fig. 5 the intensity profiles of the guided mode in the x - and z -direction are shown and compared to those of a standard telecom fiber (mode field diameter of 10.4 μm). It can be appreciated that the mode matching is good and results in theoretical coupling losses (estimated by the modes overlap) of about 1 dB/facet.

The insertion losses measured for this waveguide, coupled to standard telecom fibers, are about 4.2 dB for a sample length of 1.9 cm. Considering the above mentioned theoretical coupling losses, we can estimate an upper value for the propagation losses of 1.2 dB/cm. This is at present the best value for waveguides written in fused silica at 1 μm with the fundamental wavelength, and, in terms of insertion losses, this waveguide is also comparable to those fabricated with the second harmonic [16]. The use of the second harmonic has proved to be beneficial for fused silica to increase the nonlinear absorption, due to its large bandgap. In the present work, however, the available power at the fundamental wavelength is much higher (1.6 W overall, corresponding to 0.5 W in each of the two foci) and thus a sufficient absorption is obtained without the need for frequency doubling.

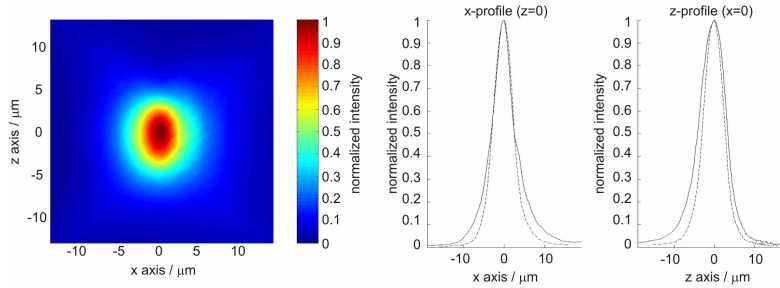


Fig. 5. Left panel: guided mode near field of one of the waveguides shown in Fig.3.1; fabrication parameters: 500 nJ and 500 $\mu\text{m/s}$. Right panel: intensity profiles in the x - and z -axis; comparison between the waveguide mode (solid line) and that of a standard telecom fiber (dashed line).

In order to evaluate the uniformity of the waveguides fabricated simultaneously by the two foci, we repeated the same measurements on each waveguide for several pairs. The mode field diameters of the two guided modes are equal within 2 % while the insertion losses differ of less than 0.5 dB.

3.2. Directional coupler written in a single sweep

When two waveguides are created in close proximity, the guided mode in one of the waveguides couples light through the evanescent field into the other waveguide, according to the coupled mode theory (see e.g. [19]). The coupling efficiency mainly depends on two parameters, the coupling coefficient C and the mismatch in the propagation constants $\Delta\beta = \beta_1 - \beta_2$. The coupling coefficient C is proportional to the overlap integral of the eigenmodes in both waveguides and increases by decreasing waveguide separation; since the guided modes overlap in their evanescent tails, the coupling coefficient is highly sensitive to the distance between the waveguides. On the other hand, the mismatch $\Delta\beta$ is zero for identical waveguides, while it increases with differences in the refractive index structure between the waveguides. Equation (1) describes the power evolution $P_1(z), P_2(z)$ in both waveguides with $P_1(0) = P_0, P_2(0) = 0$.

$$\begin{aligned} \frac{P_1(z)}{P_0} &= \cos^2(\gamma z) + \left(\frac{\Delta\beta}{2\gamma}\right)^2 \sin^2(\gamma z) \\ \frac{P_2(z)}{P_0} &= \frac{C^2}{\gamma^2} \sin^2(\gamma z) \quad \text{with} \quad \gamma^2 = C^2 + \left(\frac{\Delta\beta}{2}\right)^2 \end{aligned} \quad (1)$$

The power is oscillating along the propagation distance z with an oscillation period length determined by γ . The amount of power transfer from one waveguide to the other is called the coupling ratio; for $\Delta\beta = 0$ the power is transferred with a coupling ratio of 100 % after a length of $L_0 = \pi/2C$, while lower coupling ratios are obtained for increasing mismatch.

It is worth noting that for a fine and reproducible control of the coupler performance, it is very important to obtain exact spacing and equal refractive index profile between the two coupled waveguides. While this is easily achieved with standard photolithographic fabrication techniques, it is rather complicated with femtosecond laser writing where a double scan approach is usually employed. In fact, with the double scan approach the distance accuracy between the waveguides relies on the reproducibility of the micropositioning system; in addition writing one waveguide after the other may result in different optical properties in particular when the distance is small, since the second waveguide is partially fabricated on an already modified

region. Both these aspects are particularly limiting when very short devices (and thus highly coupled waveguides) are required and can be overcome with the present approach.

To create a directional coupler in a single sweep, we extended the multiple foci writing from a static to a moving focus scheme, where the position of the waveguides is dynamically changed during the substrate movement. In this work, we concentrate on the demonstration of X-couplers. Figure 6 illustrates the coupler layout. At section 1 and 5 the waveguides are parallel to each other, as well as in the interaction region in the center, section 3. In sections 2 and 4 the waveguides are converging/diverging following straight lines. The lengths of section 1 and 5 are chosen as 1 mm, the interaction length (section 3) as 2 mm and the lengths of sections 2 and 4 as 8 mm. Different couplers were created by varying the starting and center separation distance of the waveguides.

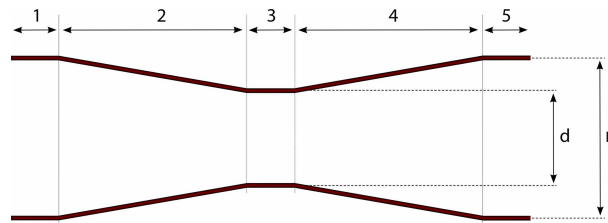


Fig. 6. Coupler Setup. The variables D and d indicate the maximum and minimum separation. See text for a detailed description of the coupler layout.

The dynamic variation of the waveguide separation requires a time-varying phase mask. Due to the finite response times of the pixels going from zero to π phase level with rise and fall times between < 190 ms (rise) and < 330 ms (fall), undefined and undesired diffraction occurs during the pixel adaption. To minimize this problem, we implemented a smooth change of the phase grating structure, as is shown in Fig. 7. The left hand side displays the grating evolution of a coupler structure (the section numbers are on top). The resulting foci distribution in the Fourier plane is pictured on the right hand side. Several orders of diffraction are present but only the ± 1 are intense enough to produce material modification.

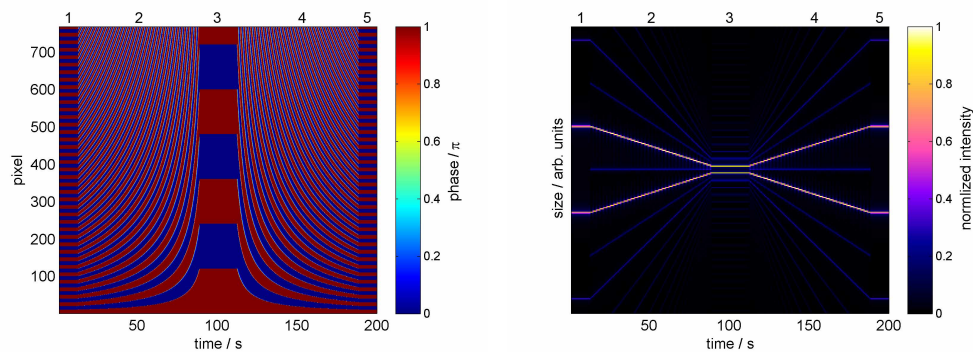


Fig. 7. Left panel: simulated phase variation applied to the SLM for the coupler fabrication. Right panel: simulation by the Fourier transform of each grating in steps of 10 ms of the time dependent position of the different foci. Numbers 1 to 5 indicate the sections introduced in Fig. 6.

With this method we have written several different coupler structures in fused silica in a single sweep at a translation speed of $100 \mu\text{m/s}$. At 20 Hz frame rate we could apply about 200

different phase masks over the length of 1 mm. Microscope images of the fabricated couplers were taken in steps of $500\ \mu\text{m}$. To visualize the full coupler these images were stitched together and then rescaled in length by a factor of 20. Figure 8 shows some examples of different couplers. The oscillating brightness of the background is due to an inhomogeneous illumination of the single microscope image, also evident in pictures of Fig. 3.

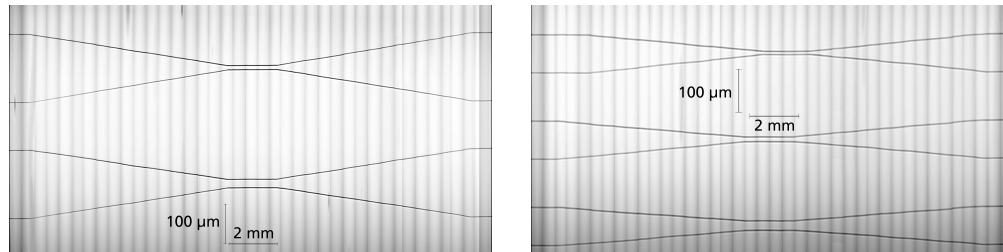


Fig. 8. Microscope images of the couplers written in glass. The image is composed by stitching together several images, each scaled down in width by a factor of 20. The image on the left shows couplers with an outer separation of $175\ \mu\text{m}$ and a center separation of $11\ \mu\text{m}$ and $22\ \mu\text{m}$. The image on the right shows couplers with an outer separation of $88\ \mu\text{m}$ and center separations of $8\ \mu\text{m}$, $11\ \mu\text{m}$ and $22\ \mu\text{m}$.

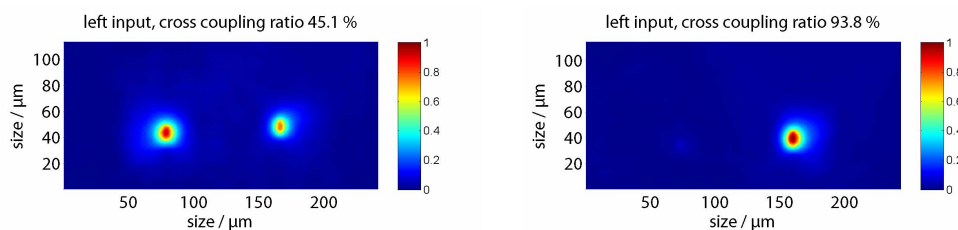


Fig. 9. Near fields of the coupler outputs with light launched into the left waveguide. The writing parameters were $500\ \text{nJ}$ per waveguide and $100\ \mu\text{m/s}$. Left panel: coupler with center separation of $11\ \mu\text{m}$. The cross-coupling-ratio is 45% . Right panel: coupler with center separation of $8\ \mu\text{m}$. The cross-coupling-ratio is 94% .

We investigated the coupling properties with a low power infrared laser and a Vidicon camera. Figure 9 shows the guided mode picture for two couplers with an input distance of $88\ \mu\text{m}$ decreasing to $11\ \mu\text{m}$ (left) and $8\ \mu\text{m}$ (right) in the center, respectively. With different center separations the coupling ratio varied between zero and almost 100% . The coupling coefficient C increases with decreasing separation between the two waveguides, which leads to an increasing oscillation frequency γ of the power exchange, and thus to different coupling ratios for a fixed wavelength and interaction length (Fig. 9). However, the observation of a coupling ratio close to 100% indicates that the mismatch $\Delta\beta$ in Eq. (1) is negligible and thus the guiding properties of both waveguides are rather equal. A systematic evaluation on the dependence of the coupler performance on the coupling length, the waveguide separation, and the wavelength will be the subject of future investigations.

4. Conclusion

We demonstrated simultaneously written waveguide pairs in fused silica with different separations. The splitting of the laser beam into two foci was realized by a phase grating from a

computer programmable beam shaper. With this technique, small waveguide separations can be controlled very precisely. By dynamic variation of the phase grating period during the substrate translation we demonstrated the creation of waveguide coupling devices with single mode guiding and variable coupling ratio for light at 1550 nm. This technique opens up a new avenue for flexible, precise and reproducible manufacturing of photonic devices such as couplers, splitters, and interferometers.

Acknowledgments

This work was supported by the European Union within contract no. IST-2005-034562 (Hybrid integrated bio-photonic sensors created by ultrafast laser systems - HIBISCUS).